Journal of Alloys and Compounds 506 (2010) 917–922

Contents lists available at ScienceDirect

Journal of Alloys and Compounds

journal homepage: www.elsevier.com/locate/jallcom

The effect of Ti substitution for Cr on transport and thermoelectric properties of $CrSb_2$ at low temperatures

Haijin Li[a,b], Xiaoying Qin[b,*], Yi Liu[a], Di Li[b]

[a] School of Mathematics and Physics, Anhui University of Technology, 243002 Ma'anshan, PR China
[b] Key Laboratory of Materials Physics, Institute of Solid State Physics, Chinese Academy of Sciences, 230031 Hefei, PR China

ARTICLE INFO

Article history:
Received 8 April 2010
Received in revised form 14 July 2010
Accepted 14 July 2010
Available online 21 July 2010

Keywords:
$Cr_{1-x}Ti_xSb_2$
Resistivity
Thermopower
Thermal conductivity

ABSTRACT

Substitutional compounds $Cr_{1-x}Ti_xSb_2$ ($0 \le x \le 0.10$) were synthesized, and the effect of Ti substitution on transport and thermoelectric properties of $Cr_{1-x}Ti_xSb_2$ were investigated from 7 to 310 K. The results indicated that the temperature dependence of electrical resistivity and thermopower $|S|$ for $CrSb_2$ did not alter significantly after substitution. However, the magnitudes of the resistivity and thermopower of $Cr_{1-x}Ti_xSb_2$ decreased monotonically with increasing Ti content owing to an increase in electron concentration indirectly caused by Ti substitution for Cr. Experiments also showed that the low-temperature lattice thermal conductivity of $Cr_{1-x}Ti_xSb_2$ generally decreased with increasing Ti content, which could originate from an enhancement of phonon scattering by increased number of Ti atoms. As a result, the figures of merit, ZT, of lightly-doped $Cr_{1-x}Ti_xSb_2$ ($x = 0.03$) samples was improved at $T > \sim 200$ K. Specifically, at 310 K, the ZT value of $Cr_{0.97}Ti_{0.03}Sb_2$ was ~11% larger than that of $CrSb_2$, indicating that thermoelectric properties of $CrSb_2$ can be improved by an appropriate substitution of Ti for Cr.

1. Introduction

Thermoelectric (TE) materials have attracted a great deal of attention in the past decade for their potential applications to refrigerators and electric-power generators [1]. The conversion efficiency of thermoelectric materials is represented by the dimensionless figure of merit, ZT ($ZT = S^2T/\rho\kappa$, where S, ρ, κ and T are the thermopower, the electrical resistivity, the thermal conductivity and the absolute temperature, respectively). A good thermoelectric material should have a high S, and low κ and ρ values. Several classes of materials are currently under investigation. These include Bi–Sb–Te-based materials [2–4], PbTe-based materials [5–7], Zn_4Sb_3-based materials [8,9], Heusler alloys [10,11], skutterudites [12,13], metal oxides [14,15], clathrate compounds [16], and pentatellurides [17]. However, the current performance of even state-of-the-art thermoelectric materials does not meet the requirements of large-scale industrial applications. The explorations of new thermoelectric materials with better performance are of great importance to future applications.

Some studies have reported that $CrSb_2$ is an important component of Li batteries [18,19]. Recent studies have investigated the potential of $CrSb_2$ as a thermoelectric material because of its high thermopower (~$|-431|\ \mu V\ K^{-1}$ at ~60 K) [20]. According to the previous work [21], $CrSb_2$ has the orthorhombic marcasite structure (crystal group *Pnnm*): each Cr atom has a distorted octahedral coordination of six nearest-neighbor Sb atoms; each Sb atom is tetrahedrally coordinated by three Cr atoms and one Sb atom, which needs 14 electrons to form the covalent bond. Therefore, the left two unpaired electrons of each Cr atom do not participate in the covalent bonding. Thus $CrSb_2$ has a d-state manifold per Cr atom $3d^2$ in $CrSb_6$-octahedron [22–24], taking a localized high-spin configuration [23]. Moreover, $CrSb_2$ is an anti-ferromagnetic compound with the Neel temperature of $T_N = 273 \pm 2$ K [25]. The magnetic properties of $Cr_{1-x}Fe_xSb_2$ ($0 \le x \le 1$) were reported by Kjekshus et al. [26], which showed that its Neel temperature decreased monotonically with increasing Fe content and diminished to zero at about $x = 0.5$. Harada et al. have reported the neutron diffraction properties of $Cr_{1-x}Ru_xSb_2$ ($x = 0.05$ and 0.2) at low temperatures [27], which presented that the magnetic unit cell of $CrSb_2$ required doubling of the b and c axes of the orthorhombic chemical cell. Furthermore, Takahashi et al. have studied the electrical resistivity ρ and magnetic properties of $Cr_{1-x}Ru_xSb_2$ ($x = 0$ and 0.1) [28]. Their results showed that in the plot of $\ln\rho$ versus $1000/T$ for $CrSb_2$ there was a plateau located in the temperature range from 50 to 80 K; correspondingly a sharp peak appeared at ~55 K in the plot of magnetic susceptibility χ versus temperature, implying that an electronic change occurred in the electron–spin system. Besides, the absolute thermopower of $Cr_{1-x}Ru_xSb_2$ alloys ($0 \le x \le 1$) increased from $|-62|\ \mu V\ K^{-1}$ to $|-252|\ \mu V\ K^{-1}$ at 300 K by the substitution of Ru for Cr; and the room-temperature resistiv-

* Corresponding author. Tel.: +86 551 5592750; fax: +86 551 5591434.
E-mail address: xyqin@issp.ac.cn (X. Qin).

0925-8388/$ – see front matter © 2010 Elsevier B.V. All rights reserved.
doi:10.1016/j.jallcom.2010.07.116

ity of $Cr_{1-x}Ru_xSb_2$ also increased with increasing Ru content [29]. In addition, the Hall coefficient (R_H) of $CrSb_2$ changed signs from negative to positive with increases in temperature from approximately 80 to 180 K [29]. On the other hand, the electrical resistance measurements conducted by Adachi et al. [22] and Harada et al. [29] showed that $CrSb_2$ is a narrow-gap semiconductor with an energy gap of 0.07 eV, which suggests that $CrSb_2$ system would be a potential candidate for thermoelectric applications. Recently, we have studied the effect of Te and Sn substitution for Sb on the transport and thermoelectric properties of $CrSb_{2-x}Te_x$ (n-type doping) [20] and $CrSb_{2-x}Sn_x$ (p-type doping) [30], respectively. After substituting Te for Sb, the *ZT* of properly-doped $CrSb_{2-x}Te_x$ compounds were improved due to the decrease in the resistivity and the thermal conductivity. Specifically, at 310 K the *ZT* of $CrSb_{1.97}Te_{0.03}$ was ~27% higher than that of $CrSb_2$ [20]. However, the thermoelectric properties of $CrSb_{2-x}Sn_x$ were not optimized due to the decrease in the thermoelectric power factor ($PF = S^2T/\rho$) [30]. In comparison with the substitution of Te and Sn for Sb, substitutional compounds $Cr_{1-x}Mn_xSb_2$ ($0 \le x \le 0.05$) were prepared and their thermoelectric properties were investigated from 7 to 310 K [31], which showed that electrical resistivity and thermal conductivity decreased with increasing Mn content, and *ZT* was improved after proper Mn substitution. For instance, the *ZT* value of $Cr_{0.95}Mn_{0.05}Sb_2$ at 310 K was ~14% higher than that of $CrSb_2$, indicating that the thermoelectric properties of $CrSb_2$ can be improved when an appropriate element is used to dope the compound and replace Cr elements. In this work, instead of substituting Mn for Cr [31], or n-type doping, we investigate the effect of substituting Group 4 elements for Cr (i.e., p-type doping) on the transport and thermoelectric properties of $CrSb_2$. Specifically, Ti-doped compounds ($Cr_{1-x}Ti_xSb_2$) were prepared, and their electrical resistivity, thermopower, and thermal conductivity were investigated in the temperature range of 7–310 K.

2. Experimental methods

Polycrystalline samples of $Cr_{1-x}Ti_xSb_2$ ($x = 0, 0.03, 0.05, 0.10$) were synthesized by using the following procedures. The mixtures of constituent elements Cr (purity: 99.9 at.%), Sb (purity: 99.9 at.%), and Ti (purity: 99.9 at.%) in stoichiometric proportions were sealed in evacuated quartz tubes under $\sim 2 \times 10^{-2}$ Pa pressure. Then they were heated slowly to 650 °C and isothermally kept for seven days to form $Cr_{1-x}Ti_xSb_2$ compounds. The phase structure of the obtained samples was examined using X-ray diffraction (XRD, Philips X'Pert Pro) with Cu Kα irradiation. Accurate lattice parameters were determined from *d*-values of XRD peaks using the standard least-squares refinement method with an Si standard for calibration. To measure their transport properties, the synthesized $Cr_{1-x}Ti_xSb_2$ powders were compacted by hot pressing (under the pressure of 300 MPa) in vacuum at 400 °C for 60 min to form bulk samples. Bar-shaped ~10 mm × ~3 mm × ~1.5 mm sized specimens were obtained from the bulk samples. Next, all transport properties (resistivity, thermopower, and thermal conductivity) were measured simultaneously using a physical property measurement system (PPMS, Quantum Design, USA) in the temperature range from 7 to 310 K. The carrier concentration was determined by measurements of the Hall coefficient at room temperature in a field, $H = 0.73T$.

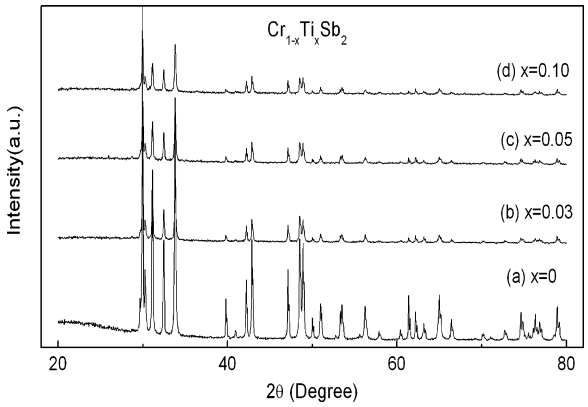

Fig. 1. XRD patterns (Cu Kα irradiation) for $Cr_{1-x}Ti_xSb_2$ ($x = 0$, 0.03, 0.05, and 0.10) at room-temperature.

3. Results and discussion

3.1. Phase determination and measurements of lattice parameters after Ti substitution

The XRD patterns of the $Cr_{1-x}Ti_xSb_2$ samples are shown in Fig. 1. It can be seen from curve (a) that all the main diffraction peaks correspond to those of standard JCPDS card of $CrSb_2$ with orthorhombic marcasite structure (crystal group *Pnnm*). As com-

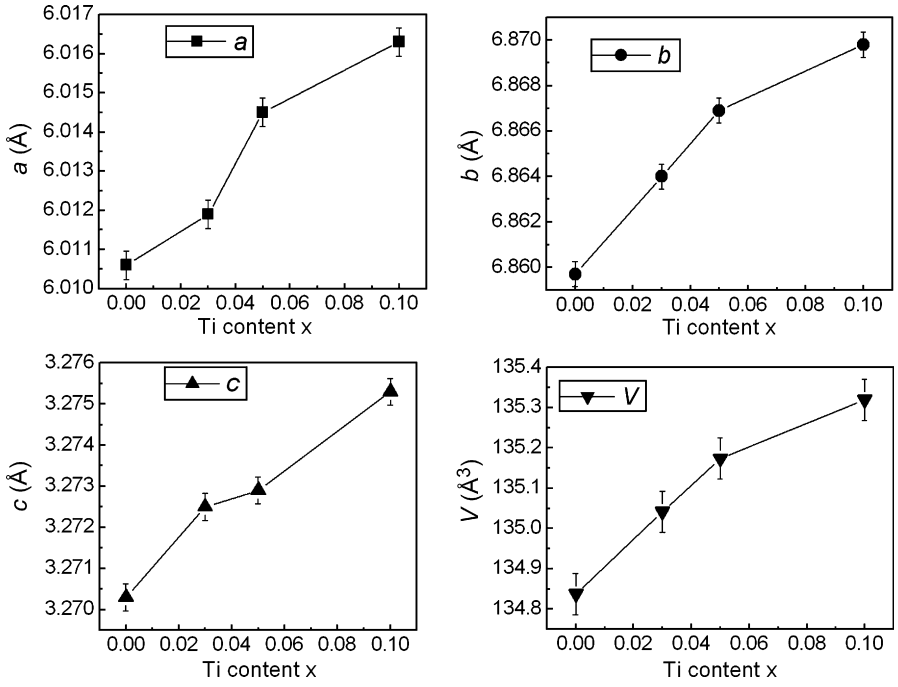

Fig. 2. Composition (x) dependence of lattice parameters *a*, *b*, *c* and volume of unit cell *V* for $Cr_{1-x}Ti_xSb_2$ ($x = 0$, 0.03, 0.05, and 0.10) at room temperature.

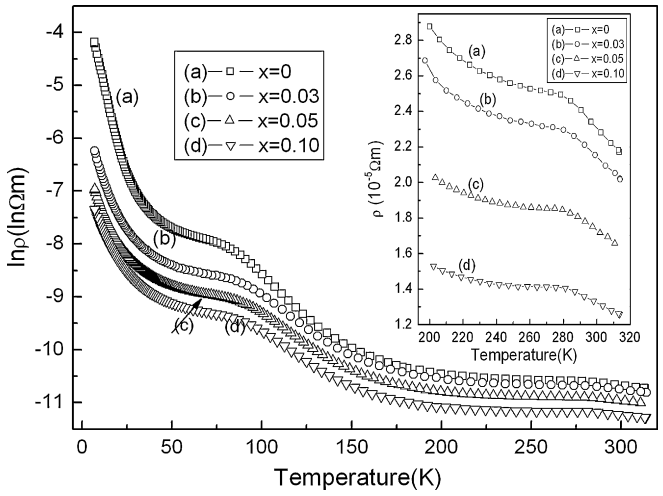

Fig. 3. Plot of the electrical resistivity ln ρ versus temperature T for $Cr_{1-x}Ti_xSb_2$ (x = 0, 0.03, 0.05, and 0.10). The inset shows variation of the electrical resistivity ρ with temperature T for $Cr_{1-x}Ti_xSb_2$ above 200 K.

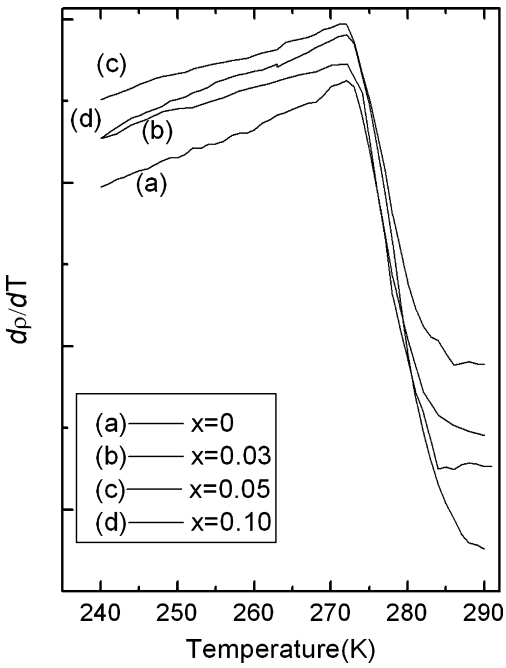

Fig. 4. Plot of dρ/dT versus T for $Cr_{1-x}Ti_xSb_2$ (x = 0, 0.03, 0.05, and 0.10) above 200 K.

pared with that of pristine $CrSb_2$, no obvious changes are observed in the XRD patterns of the doped samples. The values of lattice parameters of $Cr_{1-x}Ti_xSb_2$ are calculated using the XRD data. As shown in Fig. 2, the lattice parameters a, b, c and the volume of unit cell V of $Cr_{1-x}Ti_xSb_2$ increase monotonically with increasing Ti content due to the larger covalent radius of Ti (1.32 Å) than that of Cr (1.18 Å). These results indicate that Ti has been successfully substituted for Cr, leading to the formation of $Cr_{1-x}Ti_xSb_2$ compounds.

3.2. Effect of Ti doping on electrical resistivity and thermopower

Fig. 3 shows the temperature dependence of the electrical resistivity (plotted as ln ρ versus T) for $Cr_{1-x}Ti_xSb_2$ at temperatures ranging from 7 to 310 K (the inset, plotted as ρ versus T, presents the electrical resistivity as a function of temperature for $Cr_{1-x}Ti_xSb_2$ above 200 K). As shown in Fig. 3, the temperature dependence of electrical resistivity of $Cr_{1-x}Ti_xSb_2$ exhibits semiconductor-like behavior (i.e., dρ/dT < 0) in the whole temperature range investigated. Nevertheless, the electrical resistivity ρ of $Cr_{1-x}Ti_xSb_2$ decreases continuously with increasing Ti content. At 300 K, for instance, ρ decreases from 2.31×10^{-5} Ωm for x = 0, to 2.14×10^{-5} Ωm for x = 0.03, to 1.73×10^{-5} Ωm for x = 0.05, and finally to 1.32×10^{-5} Ωm for x = 0.10 (as shown in Table 1). Specially, a plateau in the ln ρ–T curve of $CrSb_2$ (Fig. 3) appears at the temperatures from 50 to 80 K, and an anomaly is observed markedly at about 273 K (onset temperature) (the inset in Fig. 3), which is well consistent with previous results reported by other authors [25,29]. The observed anomaly was proved to originate from anti-ferromagnetic transition [23,25,26], and the plateau was related to the electronic change in the electron–spin system of the anti-ferromagnetic semiconductor [28]. Furthermore, the plateau and anomaly (Fig. 3) also exist within the same temperature range (Fig. 4, $\Delta T_N \leq \sim 1$ K), suggesting that both the electronic change (at 50–80 K) and the Neel temperature (~273 K) are not affected significantly by Ti substitution. This system is different from Mn-doped compounds, where the Neel temperature shifted to higher temperatures with increasing Mn content, and the plateau was suppressed simultaneously [31]. According to the previous study [21–24], there are no unpaired electrons in the Ti d-orbital after substitution, which could be regarded as neutral particles, leading to little influence on the magnetic moment of Cr. As a result, there is little change in the Neel temperature of Ti-doped compounds.

In order to examine the temperature behavior of the resistivity for $Cr_{1-x}Ti_xSb_2$, logarithm of resistivity ln ρ is plotted as a function of T^{-1} in Fig. 5. One can describe their resistivity using a thermally activated form in the corresponding temperature regions, written as:

$$\rho = \rho_0 \exp\left(\frac{\Delta E}{\kappa_B T}\right) \quad (1)$$

where ρ_0 is the pre-exponential factor, ΔE is the activation energy for conduction, and κ_B is the Boltzmann constant. The best fit for the experimental data following Eq. (1) yields four activation energies ΔE_i (i = 1, 2, 3, 4) (Fig. 6). The activation energies ΔE_i (i = 1, 2, 3, 4) values for $CrSb_2$ are 32.6 (~276 K < T < ~310 K), 35.7 (~60 K < T < ~276 K), 4.6 (~12 K < T < ~60 K), and 0.9 meV (~7 K < T < ~12 K), respectively. The value of ΔE_2 is about half of the energy gap (E_g), or 0.07 eV, which is consistent with results reported by Adachi et al. [22] and Harada et al. [29]. As plotted in Fig. 6, ΔE_1 is smaller than ΔE_2 for $Cr_{1-x}Ti_xSb_2$, which may be caused by the transition from anti-ferromagnetism to paramagnetism. In comparison, ΔE_3 and ΔE_4 are much smaller than ΔE_2 (or the E_g), indicating that they can be attributed to impurity or defect levels. According to the covalent bonding model [21–24], the substitution of Cr ([Ar]3d^{5}4s^1) by Ti ([Ar]3d^{2}4s^2) in $CrSb_2$ would introduce acceptor levels (or impurity states) into the energy gap of the host, which will lead to a decrease in electron concentration due to compensation effect in this n-type semiconductor (as proved by negative value of its thermopower, Fig. 7), giving rising to an increase in the resistivity. On the other hand, however, Ti doping may cause shifts in impurity or defect levels, or even changes in the band gap. In fact, the monotonic decrease in the activation energies ΔE_i (i = 1, 2, 3) with increasing Ti content (Fig. 6) suggests a shift in impurity or defect levels toward the edge of the conduction band(s)

Table 1
Hall coefficient R_H, carrier contention n_c, resistivity ρ of $Cr_{1-x}Ti_xSb_2$ ($0 \leq x \leq 0.10$) at room temperature.

Composition (x)	0	0.03	0.05	0.10
R_H (cm^3 C^{-1})	−0.48	−0.39	−0.33	−0.16
n_c (10^{21} cm^{-3})	1.31	1.61	1.89	2.32
ρ (10^{-5} Ωm)	2.31	2.14	1.73	1.32

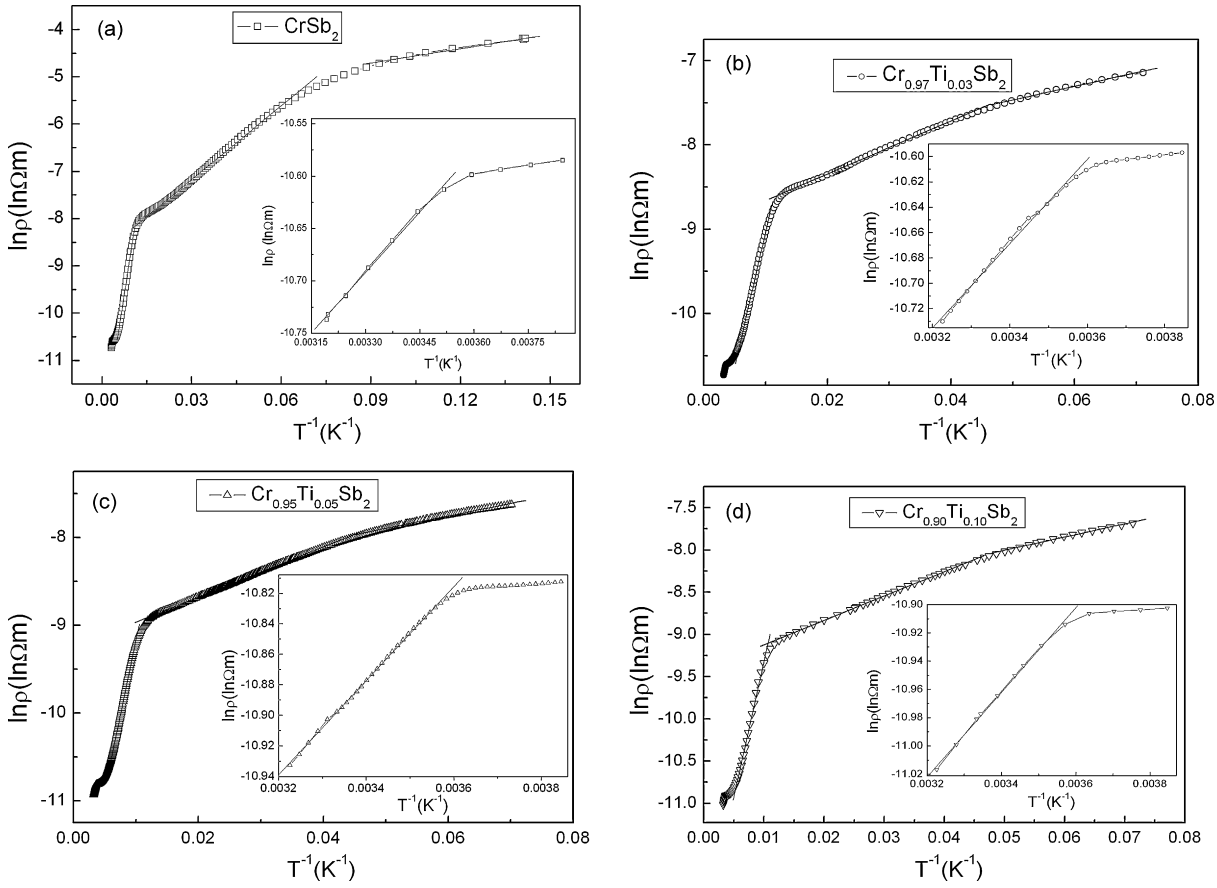

Fig. 5. Plot of ln ρ versus T^{-1} for $Cr_{1-x}Ti_xSb_2$ (x = 0, 0.03, 0.05, and 0.10): (a) for $CrSb_2$, (b) for $Cr_{0.97}Ti_{0.03}Sb_2$, (c) for $Cr_{0.95}Ti_{0.05}Sb_2$, (d) for $Cr_{0.90}Ti_{0.10}Sb_2$.

or even a narrowing of the energy gap would occur because of lattice distortion (Fig. 2), which should result in an increase in electron concentration. In fact, room-temperature measurements of the R_H indicate that the electron concentration increases monotonically from 1.31×10^{21} cm^{-3} for x = 0 to 2.32×10^{21} cm^{-3} for x = 0.10 (Table 1). Therefore, narrowing of the energy gap and/or shifts in impurity (or defect) levels could be the major effects of doping, and these could be the underlying cause of the decrease in the resistivity of $Cr_{1-x}Ti_xSb_2$ compounds (Fig. 3) with increasing Ti doping content.

Fig. 7 gives the thermopower as a function of temperature for $Cr_{1-x}Ti_xSb_2$. The thermopower for all the samples are negative, indicating that electrons are the major charge carriers in these compounds over the entire temperature range. The absolute values of the thermopower, $|S|$, for $CrSb_2$ first increase from $|-42|$ to $|-431|$ μV K^{-1} with increasing temperature, and then $|S|$ decreases to $|-75|$ μV K^{-1} with further increasing in temperature to 310 K, leaving a large peak at ~60 K. By comparing Fig. 3 with Fig. 7, the large peak in the plot of S versus T for $CrSb_2$ corresponds to the plateau in the ln ρ versus T curve, suggesting strongly that they are

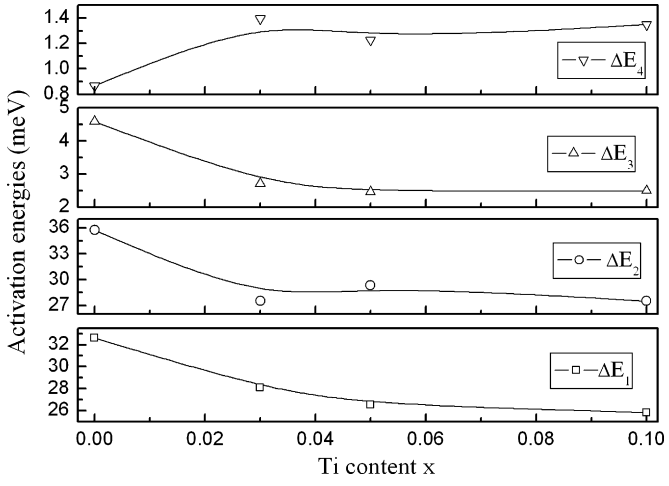

Fig. 6. Variation of the activation energies ΔE_i (i = 1, 2, 3, 4) with the Ti content x for $Cr_{1-x}Ti_xSb_2$ (x = 0, 0.03, 0.05, and 0.10).

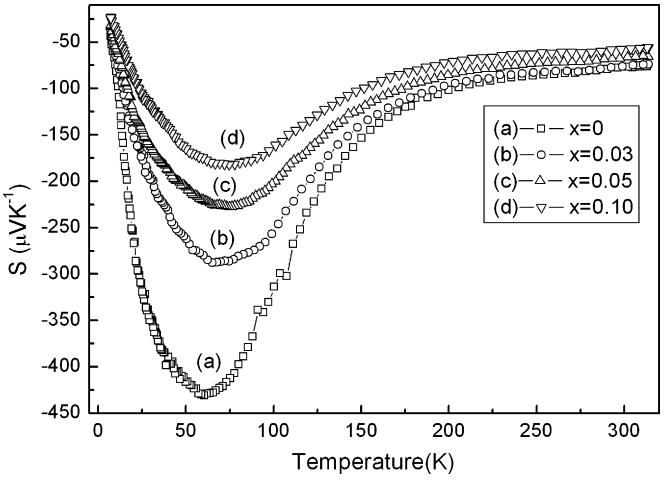

Fig. 7. Variation of the thermopower S with temperature T for $Cr_{1-x}Ti_xSb_2$ (x = 0, 0.03, 0.05, and 0.10).

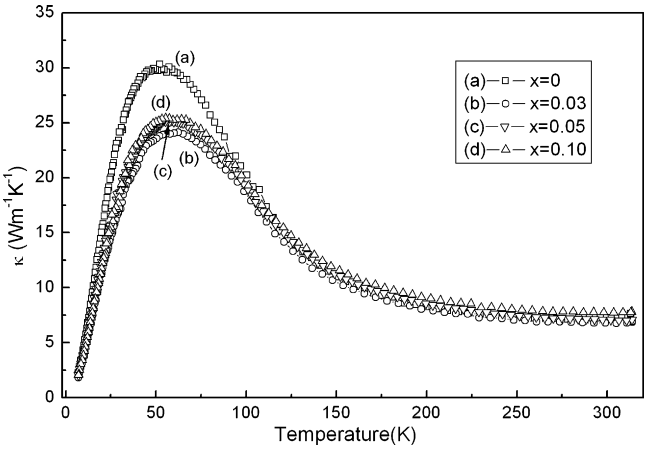

Fig. 8. Plot of thermal conductivity κ versus temperature T for $Cr_{1-x}Ti_xSb_2$ ($x = 0$, 0.03, 0.05, and 0.10).

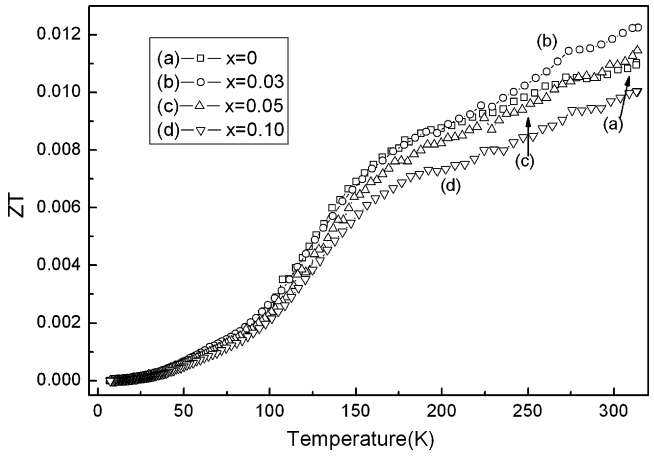

Fig. 10. Variation of ZT with temperature T for $Cr_{1-x}Ti_xSb_2$ ($x = 0$, 0.03, 0.05, and 0.10).

correlated to each other. The large peak value ($-431\ \mu V\,K^{-1}$) of S is also related to the electronic change of the electron–spin system. In comparison, $|S|$ decreases obviously with increasing Ti content over the entire temperature range, which could be caused by an increase in electron concentration due to the substitution of Ti for Cr, as discussed above.

3.3. Effect of doping with Ti on thermal conductivity and figure of merit

Fig. 8 presents the total thermal conductivities of the $Cr_{1-x}Ti_xSb_2$ ($x = 0$, 0.03, 0.05, and 0.10) compounds. As shown in Fig. 8, the thermal conductivities of all the samples increase with increasing temperature, reach a maximum value, and then decrease with further increasing temperature. The maximum values of the thermal conductivity may obtain when phonon–phonon umklapp scattering becomes important [32]. The total thermal conductivity (κ) may be expressed as the sum of the lattice component (κ_L) and the carrier component (κ_C): $\kappa = \kappa_L + \kappa_C$. The κ_C values can be estimated from Wiedemann–Franz's law as $\kappa_C = LT/\rho$, where L is the Lorentz number and ρ is the electrical resistivity. As a semi-quantitative estimation, we use the value L_0 of free electrons for L (i.e. $L = L_0 = 2.44 \times 10^{-8}\ V^2/K^2$) for all the samples. Consequently, the lattice thermal conductivity (κ_L) can be obtained from κ and κ_C (inset of Fig. 9), as shown in Fig. 9. By comparing Fig. 8 with Fig. 9, it can be seen that the thermal conductivities of all compounds arise mainly from their lattice thermal conductivities. At high temperatures ($T > \sim 100$ K), no large differences in lattice thermal conductivities are observed among $Cr_{1-x}Ti_xSb_2$ compounds with different values of x (Fig. 9). Nevertheless, compared to those of $CrSb_2$, the lattice thermal conductivities of the doped samples decrease substantially at temperatures below ~100 K, which could be attributed to the enhanced phonon scattering by impurity (Ti) atoms. The lattice thermal conductivity of a lightly-doped sample is smaller than that of a heavily-doped sample at low temperatures due to the specific location or distribution of Ti atoms in the host. The more random distribution of Ti atoms in the host lattice, in the case of light doping, leading to stronger phonon scattering, the lower lattice thermal conductivity is. Nevertheless, the exact underlying mechanism needs to be elucidated by more elaborate experiments.

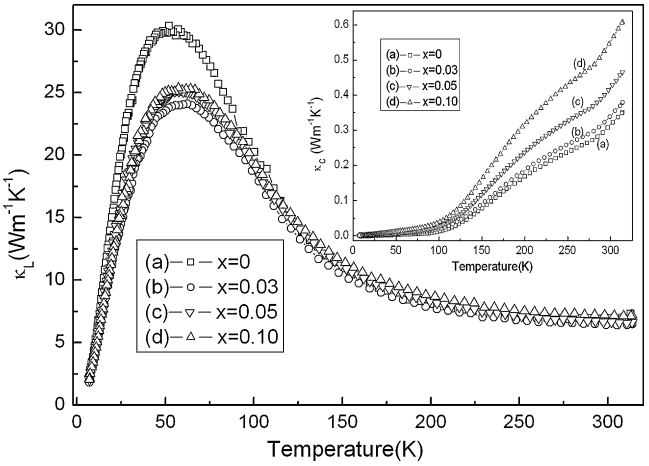

Fig. 9. Plot of lattice thermal conductivity κ_L versus temperature T for $Cr_{1-x}Ti_xSb_2$ ($x = 0$, 0.03, 0.05, and 0.10). The inset shows the variation of carriers' thermal conductivity κ_C with temperature T for $Cr_{1-x}Ti_xSb_2$.

The figure of merit ZT values of $Cr_{1-x}Ti_xSb_2$ are calculated and presented as a function of temperature in Fig. 10. The ZT values for all the samples increase monotonically with increasing temperature. Above ~200 K, the ZT values of lightly-doped $Cr_{1-x}Ti_xSb_2$ compounds ($x = 0.03$) are larger than those of other compounds. Specifically, the ZT value for $Cr_{0.97}Ti_{0.03}Sb_2$ is ~0.012 at 310 K, which is about 11% larger than that of $CrSb_2$, indicating that thermoelectric properties of $CrSb_2$ can be optimized by proper substitution of Ti for Cr.

4. Conclusions

Substituted compounds $Cr_{1-x}Ti_xSb_2$ were synthesized, and the effect of Ti substitution on the transport and thermoelectric properties of $Cr_{1-x}Ti_xSb_2$ was investigated at temperatures below 310 K. The results indicated that the temperature dependence of electrical resistivity and thermopower of $CrSb_2$ were not markedly altered by substitution of Cr by Ti. However, the magnitudes of the resistivity and thermopower of $Cr_{1-x}Ti_xSb_2$ decreased monotonically with increasing Ti content. This could be explained by the increase in electron concentration due to Ti substitution for Cr. In addition, experiments shown that low-temperature lattice thermal conductivity (below ~100 K) of $Cr_{1-x}Ti_xSb_2$ generally decreased presumably due to enhanced phonon scattering by doped Ti atoms. Moreover, the ZT values of doped compound $Cr_{0.97}Ti_{0.03}Sb_2$ were larger than those of un-doped $CrSb_2$ because of decreased resistivity after doping, indicating that the thermoelectric properties $CrSb_2$ may be improved by substitution of Ti for Cr.

Acknowledgement

Financial support from National Natural Science Foundation of China (Grants No. 10774145, No. 50701043, No. 10904144 and No. 50972146) is gratefully acknowledged.

References

[1] F.J. DiSalvo, Science 285 (1999) 703.
[2] C.N. Liao, L.C. Wu, J.S. Lee, J. Alloys Compd. 490 (2010) 468.
[3] C.H. Kuo, C.S. Hwang, M.S. Jeng, W.S. Su, Y.W. Chou, J.R. Ku, J. Alloys Compd. 496 (2010) 687.
[4] Y.S. Hor, R.J. Cava, J. Alloys Compd. 479 (2009) 368.
[5] T.C. Su, X.P. Jia, H.A. Ma, J.G. Guo, Y.P. Jiang, N. Dong, L. Deng, X.B. Zhao, T.J. Zhu, C. Wei, J. Alloys Compd. 468 (2009) 410.
[6] K.F. Cai, C. Yan, Z.M. He, J.L. Cui, C. Stiewe, E. Müller, H. Li, J. Alloys Compd. 469 (2009) 499.
[7] T.C. Su, S.S. Li, H.A. Ma, X.L. Li, L. Deng, Y. Yan, W. Guo, X.P. Jia, J. Alloys Compd. 497 (2010) 432.
[8] J.H. Sun, X.Y. Qin, H.X. Xin, D. Li, L. Pan, C.J. Song, J. Zhang, R.R. Sun, Q.Q. Wang, Y.F. Liu, J. Alloys Compd. 500 (2010) 215.
[9] W. Li, L.M. Zhou, Y.L. Li, J. Jiang, G.J. Xu, J. Alloys Compd. 486 (2009) 335.
[10] P.J. Lee, S.C. Tseng, L.S. Chao, J. Alloys Compd. 496 (2010) 620.
[11] M. Mikami, S. Tanaka, K. Kobayashi, J. Alloys Compd. 484 (2009) 444.
[12] M. Chitroub, F. Besse, H. Scherrer, J. Alloys Compd. 467 (2009) 31.
[13] L. Zhang, A. Grytsiv, M. Kerber, P. Rogl, E. Bauer, M. Zehetbauer, J. Alloys Compd. 490 (2010) 19.
[14] L.X. Xu, F. Li, Y. Wang, J. Alloys Compd. 501 (2010) 115.
[15] J. Liu, C.L. Wang, W.B. Su, H.C. Wang, J.C. Li, J.L. Zhang, L.M. Mei, J. Alloys Compd. 492 (2010) L54.
[16] H.F. Wang, K.F. Cai, H. Li, D.H. Yu, X. Wang, C.W. Zhou, X.L. Li, Y.Y. Wang, B.J. An, Y. Du, J. Alloys Compd. 491 (2010) 684.
[17] I. Terasaki, Y. Sasago, K. Uchimokuro, Phys. Rev. B 56 (1997) R12685.
[18] C.M. Park, H.J. Sohn, Electrochim. Acta 55 (2010) 4987.
[19] F.J. Fernández-Madrigal, P. Lavela, C. Pérez-Vicente, J.L. Tirado, J. Electroanal. Chem. 501 (2001) 205.
[20] H.J. Li, X.Y. Qin, D. Li, Mater. Sci. Eng. B: Solid 149 (2008) 53.
[21] G. Brostigen, A. Kjekshus, Acta Chem. Scand. 24 (1970) 2983.
[22] K. Adachi, K. Sato, M. Matsuura, J. Phys. Soc. Jpn. 26 (1969) 906.
[23] G. Brostigen, A. Kjekshus, Acta Chem. Scand. 24 (1970) 2993.
[24] J.B. Goodenough, J. Solid State Chem. 5 (1972) 144.
[25] H. Holseth, A. Kjekshus, Acta Chem. Scand. 24 (1970) 3309.
[26] A. Kjekshus, P.G. Peterzens, T. Rakke, A.F. Andresen, Acta Chem. Scand. Ser. A 33 (1979) 469.
[27] T. Harada, Y. Takahashi, Y. Yamaguchi, T. Kanomata, H. Yoshida, T. Kaneko, Y. Kawazoe, J. Magn. Magn. Mater. 310 (2007) 1569.
[28] Y. Takahashi, T. Harada, T. Kanomata, K. Koyama, H. Yoshida, T. Kaneko, M. Motokawa, M. Kataoka, J. Alloys Compd. 459 (2008) 78.
[29] T. Harada, T. Kanomata, Y. Takahashi, O. Nashima, H. Yoshida, T. Kaneko, J. Alloys Compd. 383 (2004) 200.
[30] H.J. Li, X.Y. Qin, D. Li, H.X. Xin, J. Alloys Compd. 472 (2009) 400.
[31] H.J. Li, X.Y. Qin, D. Li, J. Alloys Compd. 467 (2009) 299.
[32] K. Berggild, M. Kriener, C. Zobel, A. Reichl, A. Freimuth, T. Lorenz, Phys. Rev. B 72 (2005) 155116.